


---

This is the **accepted version** of the journal article:

Elorza-Vidal, Xabier [et al.]. «GlialCAM/MLC1 modulates LRRC8/VRAC currents in an indirect manner : Implications for megalencephalic leukoencephalopathy». *Neurobiology of disease*, Vol. 119 (November 2018), p. 88-99 DOI 10.1016/j.nbd.2018.07.031, PMID 30076890

---

This version is available at <https://ddd.uab.cat/record/324795>

under the terms of the  <sup>IN</sup>COPYRIGHT license.

# GlialCAM/MLC1 modulates LRRC8/VRAC currents in an indirect manner: Implications for megalencephalic leukoencephalopathy

Xabier Elorza-Vidala,<sup>b,1</sup> Sònia Sirisia,<sup>1</sup> Héctor Gaitán-Peñas<sup>a,b</sup>, Carla Pérez-Riusa, Marta Alonso-Gardón<sup>a</sup>, Mercedes Armand-Ugón<sup>a</sup>, Angela Lanciottic, Maria Stefani<sup>a</sup> Brignone<sup>c</sup>, Esther Prat<sup>b,d</sup>, Virginia Nunes<sup>b,d</sup>, Elena Ambrosini<sup>c</sup>, Xavier Gasull<sup>e,f</sup>, Raúl Estévez<sup>a,b,\*</sup>

*a Unitat de Fisiologia, Departament de Ciències Fisiològiques, Genes Disease and Therapy Program IDIBELL-Institute of Neurosciences, Universitat de Barcelona, L'Hospitalet de Llobregat, Spain*

*b Centro de Investigación en red de enfermedades raras (CIBERER), ISCIII, Spain*

*c Department of Neuroscience, Istituto Superiore di Sanità, Viale Regina Elena 299, Rome 00161, Italy*

*d Unitat de Genètica, Departament de Ciències Fisiològiques, Laboratori de Genètica Molecular, Genes Disease and Therapy Program IDIBELL, Universitat de Barcelona, L'Hospitalet de Llobregat, Spain*

*e Grup de Neurofisiologia, Departament de Biomedicina, Facultat de Medicina, Institut de Neurociències, Universitat de Barcelona, Casanova 143, 08036 Barcelona, Spain*

*f Institut d'Investigacions Biomèdiques August Pi i Sunyer (IDIBAPS), 08036 Barcelona, Spain*

\*Corresponding author at: *Facultat de Medicina, Departament de Ciències Fisiològiques, Universitat de Barcelona, IDIBELL, C/Feixa Llarga s/n, 08907 L'Hospitalet de Llobregat, Barcelona, Spain.*

E-mail address: [restevez@ub.edu](mailto:restevez@ub.edu) (R. Estévez).

<sup>1</sup> Xabier Elorza-Vidal and Sònia Sirisi contributed equally to this work.

## Abstract

Megalencephalic leukoencephalopathy with subcortical cysts (MLC) is a rare type of leukodystrophy caused by mutations in either MLC1 or GLIALCAM genes. Previous work indicated that chloride currents mediated by the volume-regulated anion channel (VRAC) and CIC-2 channels were affected in astrocytes deficient in either Mlc1 or Glialcam. CIC-2 forms a ternary complex with GlialCAM and MLC1. LRRC8 proteins have been identified recently as the molecular components of VRAC, but the relationship between MLC and LRRC8 proteins is unknown. Here, we first demonstrate that LRRC8 and MLC1 are functionally linked, as MLC1 cannot potentiate VRAC currents when LRRC8A, the main subunit of VRAC, is knocked down. We determine that LRRC8A and MLC1 do not co-localize or interact and, in *Xenopus* oocytes, MLC1 does not potentiate LRRC8-mediated VRAC currents, indicating that VRAC modulation in astrocytes by MLC1 may be indirect. Investigating the mechanism of modulation, we find that a lack of MLC1 does not influence either mRNA or total and plasma membrane protein levels of LRRC8A; and neither does it affect LRRC8A subcellular localization. In agreement with recent results that indicated that overexpression of MLC1 decreases the phosphorylation of extracellular signal-regulated kinases (ERK), we find that astrocytes lacking MLC1 show an increase in ERK phosphorylation. In astrocytes with reduced or increased levels of MLC1 we observe changes in the phosphorylation state of the VRAC subunit LRRC8C. Our

results thus reinforce previous suggestions that indicated that GlialCAM/MLC1 might modify signal transduction pathways that influence the activity of different proteins, such as VRAC.

## Introduction

Megalencephalic leukoencephalopathy with subcortical cysts (MLC) is a rare type of leukodystrophy (van der Knaap et al., 2012), caused by mutations in two different genes: MLC1, which is more frequent (Leegwater et al., 2001), and GLIALCAM (Lopez-Hernandez et al., 2011a). MLC1 is a membrane protein that exhibits a low level of homology to ion channels (Estévez et al., 2018), while GlialCAM is an adhesion molecule that belongs to the immunoglobulin superfamily (Barrallo-Gimeno et al., 2015). GlialCAM is required for MLC1 endoplasmic reticulum exit and targeting to astrocyte-astrocyte junctions, as shown in rat astrocytes with reduced expression of GlialCAM and in Glialcam knockout (KO) mice (Bugiani et al., 2017; Capdevila-Nortes et al., 2013; Hoegg-Beiler et al., 2014).

Studies of a MLC patient brain biopsy revealed that myelin and astrocytes showed vacuolation (Duarri et al., 2011; van der Knaap et al., 1996). Furthermore, spectroscopic MRI studies indicated an increased water content in patients' brains (De Stefano et al., 2001). These results suggest that MLC patients present a defect in fluid homeostasis. In the same manner, histology and capacitance measurements of astrocytes and oligodendrocytes from Glialcam and Mlc1 KO mice showed that these cells were swollen and were vacuolated (Bugiani et al., 2017; Capdevila-Nortes et al., 2013; Hoegg-Beiler et al., 2014).

An important question is why are these cells swollen. As the molecular role of GlialCAM and MLC1 is still unknown, it was speculated that GlialCAM/MLC1 could influence or interact with other proteins such ion channels resulting in an altered ionic homeostasis (Brignone et al., 2015; Estévez et al., 2018; van der Knaap et al., 2012). Consistent with this hypothesis, an altered potassium homeostasis has recently been observed in Mlc1 and Glialcam KO mice (Dubey et al., 2018). Proteomic experiments aimed at finding GlialCAM-associated proteins resulted in the identification of the CIC-2 chloride channel (Jeworutzki et al., 2012). Later, it was found that CIC-2 forms a depolarization-dependent ternary complex with GlialCAM and MLC1 in astrocytes (Sirisi et al., 2017) and a binary complex with GlialCAM in oligodendrocytes (Hoegg-Beiler et al., 2014). These two complexes expressed by two different cell populations may also interact through GlialCAM-mediated trans interactions. The interaction of GlialCAM/MLC1 with CIC-2 changes CIC-2 subcellular localization (Jeworutzki et al., 2012), increases CIC-2 stability at the plasma membrane (Gaitán-Peñas et al., 2017) and modifies CIC-2 functional properties (Capdevila-Nortes et al., 2015; Jeworutzki et al., 2014). It has been suggested that the modification of CIC-2 activity by GlialCAM/MLC1 may be needed to allow chloride influx at depolarized potentials (Sirisi et al., 2017). This chloride influx may ease potassium influx in depolarized glial cells during situations of high neuronal activity, as the former may compensate the positive charge of the latter (Kofuji and Newman, 2004). Since *Clcn2*<sup>-/-</sup> mice display a similar vacuolation phenotype to that observed in MLC patients (Blanz et al., 2007), MLC1/GlialCAM mediated alterations of CIC-2 function could partially explain altered potassium and fluid homeostasis in MLC. However, the vacuolating phenotype of the double KO mice for Glialcam and *Clcn2* is more severe than the phenotype of the Glialcam KO mice (Hoegg-Beiler et al., 2014). Furthermore, mutations in *CLCN2* have

been found in a leukodystrophy exhibiting a different phenotype from that of MLC patients (Depienne et al., 2013; van der Knaap et al., 1993). Thus, it was then hypothesized that GlialCAM and MLC1 may influence other proteins related to water/ions homeostasis. Additional studies have suggested that GlialCAM/MLC1 may also regulate other proteins related to ion movement, such as Na<sup>+</sup>/K<sup>+</sup>-ATPase (Brignone et al., 2011; Sugio et al., 2017), Connexin 43 (Wu et al., 2016), V-ATPase (Brignone et al., 2014), the TRPV4 channel (Lanciotti et al., 2012) and volume-regulated anion channels (VRACs) (Capdevila-Nortes et al., 2013; Ridder et al., 2011), through unknown mechanisms.

Considering VRAC, it has been shown that in astrocyte cultures with reduced or complete absence of MLC1 or GlialCAM, and in lymphoblast from MLC patients, there is a decrease of VRAC currents (Capdevila-Nortes et al., 2013; Dubey et al., 2015; Ridder et al., 2011; Sirisi et al., 2014). Conversely, overexpression of MLC1 but not GlialCAM in primary astrocytes potentiates VRAC currents (Capdevila-Nortes et al., 2013). VRACs are a major player in volume regulation: they release osmolytes such as taurine and glutamate and anions such as chloride upon their activation induced by reduction of extracellular osmolarity or increase in intracellular osmolarity (Jentsch, 2016). This release changes the driving force of osmolarity and results in an efflux of water. This process is called regulatory volume decrease (RVD) and allows cells to restore to their original size after a hypotonic shock (Pasantes-Morales et al., 2006). RVD was also deficient in astrocytes with reduced expression of MLC1 (Ridder et al., 2011).

Recently, the proteins responsible for VRAC activity have been identified (Qiu et al., 2014; Syeda et al., 2016; Voss et al., 2014). It was found that VRAC is mediated by heteromers of the leucine-rich-repeat-containing 8, member A (LRRC8A) protein together with other members of the same family (LRRC8B, LRRC8C, LRRC8D and LRRC8E). In astrocytes, it has been shown that RNA interference of LRRC8 genes reduced the release of taurine and aspartate (Hydzinski-García et al., 2014; Schober et al., 2017). However, it remains to be demonstrated that VRAC currents depend on LRRC8 proteins in astrocytes, since they express other chloride channels, such as bestrophins, which are also involved in volume-dependent chloride currents (Kunzelmann, 2015). A very recent work has shown that LRRC8A is essential for swelling-activated chloride currents and for regulatory volume decrease in astrocytes (Formaggio et al., 2018). Here, we first corroborated that VRAC currents in astrocytes also depend on LRRC8A and then we studied the mechanism by which MLC1 modulates LRRC8/VRAC currents.

## **Methods**

### *Primary culture and adenoviral transduction*

Rat primary quiescent astrocyte cultures were prepared as described previously (Duarri et al., 2011) and maintained in culture in the presence of the mitotic inhibitor AraC. We used these cultures for biochemical studies. Dibutyryl-cAMP differentiated rat astrocytes, used for electrophysiological measurements, were obtained as described elsewhere (Ferroni et al., 1997). We used differentiated cells as these cells express CIC-2 and VRAC chloride currents and are rounded, which makes the patch pipette clamp easier. Immunofluorescence experiments were performed on both types of cultures, with similar results. The physiological solution was: (in mM) NaCl 122, KCl

3.3, MgSO<sub>4</sub> 0.4, CaCl<sub>2</sub> 1.3, KH<sub>2</sub>PO<sub>4</sub> 1.2, HEPES 25, Glucose 10, and it had pH 7.4. The osmolarity was 290–310 mOsm/kg and was adjusted with mannitol using a vapour-pressure osmometer (Model 3320, Advanced Instruments). In the hypoosmolar solution the osmolarity was adjusted to 215–230 mOsm/kg. Adenovirus expressing HA-tagged MLC1 and the transduction of astrocytes has been described previously (Jeworutzki et al., 2012; Lopez-Hernandez et al., 2011b).

#### *RNA interference*

RNAi entry-clone (Gateway, Invitrogen) vectors were prepared using the Block-it PolII miR RNAi EmGFP or the Block-it PolIII miR RNAi expression vector kit following the manufacturer's instructions. Entry clones were recombined using LR clonase into the vector pAdVDEST- CMV/V5. Adenoviruses were produced and titrated using fluorescence microscopy detecting EmGFP, which is expressed together with the shRNA, or detecting the viral protein Ad-Hexon. The adenoviruses expressed a negative control shRNA (scrambled shRNA; SCR) or shRNA directed against rat MLC1 (shRNA 905) (Capdevila-Nortes et al., 2013; Duarri et al., 2011). The sequence of the oligo used to knock down rat LRRC8A expression was: shRNA LRRC8A1 (shRNA mi2269): 5' TTCTG CAAGAGGCCAATGTCA 3'.

#### *Real-time PCR*

Total RNA was isolated with TRIzol (Life Technologies) and retro-transcribed using random hexamers with the SuperScript III system (Life Technologies). The following oligonucleotide pairs were used for qPCR (5' to 3'): AGCCACAACAACCTGACCTTCC and GGAGCGCTTCA ATCCTATTGGC (mouse *Lrrc8a*); and as an internal control: AAGTCCC TCACCCTCCCAAAG and AAGCAATGCTGTCACCTTCCC ( $\beta$ -Actin). qPCR was performed with SYBR Select reagent (Life Technologies) in a StepOne apparatus (Life Technologies). Three experiments were analysed, with three replicate samples in each experiment. The expression levels were calculated using the  $2^{-\Delta\Delta C_t}$  method and normalized to the internal control gene.

#### *Antibodies, immunofluorescence, Western blotting and biotinylation studies in astrocytes*

For immunofluorescence staining, cells were fixed and processed as previously described (Duarri et al., 2011). The polyclonal rabbit antibodies used were the following: anti-GliaCAM (1:100 (Lopez-Hernandez et al., 2011a)), anti-MLC1 (1:100, (Teijido et al., 2004)), anti-CIC-2 (1:100, (Jeworutzki et al., 2012)), and the antibody developed in this work anti-LRRC8A (1:100) against the peptide CQRTKS-RIEQGIVDRSE, using the services provided by Eurogentec or the commercially available antibody A304–175-A (1:1000) (Bethyl antibodies).

We also used a mouse monoclonal antibody that was developed against the mouse peptide sequence of the N terminus of MLC1 (TREGQFRE-ELGYDRM) (Sirisi et al., 2017).

In the Western blot studies, astrocyte lysates were prepared and processed as previously described (Duarri et al., 2011).  $\beta$ -Actin protein was used as a loading

control.

To detect surface levels of LRRC8A, rat astrocytes were cultured in 6 cm plates. They were washed 3 times with PBS-CM (PBS with 1 mM CaCl<sub>2</sub> and 1 mM MgCl<sub>2</sub>). Subsequently, the astrocytes were incubated on ice for 30 min in PBS-CM containing 2 mg/ml EZ-Link<sup>TM</sup> Sulfo-NHS- Biotin (Thermo Scientific). After 3 washes with PBS-CM, they were quenched for 10 min in PBS Ca/Mg containing 10 mM Lysine. After 3 additional washes with PBS-CM, the cells were lysed in RIPA buffer (50 mM Tris pH 8, 150 mM NaCl, 1% NP-40, 0.5% deoxycholate, 0.1% SDS, 2 mM EDTA) containing protease inhibitors, for 1 h. After centrifugation for 15 min at 14000 rpm, the lysate was quantified using the BCA protein assay (Thermo Fisher). Then 2 mg of the solubilized extract in a total volume of 200 µl was incubated with 100 µl of streptavidin agarose (Thermo Fisher) O/N at 4 °C. After a brief centrifugation, the supernatant (SN) was taken and the beads were washed three times with RIPA buffer. Biotinylated proteins were eluted with LSB 1× for 15 min at 60 °C. Samples of lysate, SN and eluate were analysed by Western blot. To confirm that only membrane proteins were detected in the eluate, we performed a Western blot with antibodies to test for the protein resident in the endoplasmic reticulum, calnexin (Genescript, 1:100).

#### *Affinity purification of LRRC8A and MS analysis of LRRC8A- associated proteins in astrocytes*

Membrane suspensions from MLC1kd (knockdown) astrocytes (100 µl) and MLC1++ (overexpression of MLC1) astrocytes (100 µl) with 0.2 mg protein each were mixed with 500 µl CLβ enhancer, incubated for 20 min and ultracentrifugated (10 min/45,000 rpm). The pellets were then solubilized with 200 µl solubilization buffer (CL47a + 50 mM NaCl, 2 mM EGTA/EDTA and protease inhibitors) for 20 min at 4 °C and ultracentrifugated (6 min at 40000 rpm). Then, 10 µg of immobilized antibody (1:1 mix of anti-LRRC8A from our own anti- body and the Bethyl antibody) was incubated with 200 µl of each solubilize (3 h/4 °C on a wheel), washed twice with 500 µl CL47a + dilution buffer and eluted with 2 × 4 µl Laemmli buffer (-DTT; 2 × 10 min/37 °C). Finally, 1 µl 1 M DTT was added to the eluates and they were incubated for 5 min at 37 °C prior to loading on SDS-PAGE (95% for MS analysis, i.e. short run and silver stained; 5%, together with 3 µl aliquots taken of the affinity purification (AP) from homogenate, solubilize, pellet and unbound fractions, resolved by SDS-PAGE and electroblotted on PVDF membranes with detection using HRP-conjugated secondary antibodies/ECL prime/Hyperfilm).

Two samples per gel lane (> and < 50 kDa) were excised and each subjected to standard in-gel tryptic digestion (Pandey et al., 2000). The peptides eluted were vacuum dried and redissolved in 13 µl 0.5% trifluoroacetic acid. For comprehensive and sensitive LC-MS/MS analysis, samples were loaded into a C18 PepMap100 precolumn (5 µm; Dionex) and resolved in an analytical 75 µm × 10 cm C18 column (PicoTip<sup>TM</sup> Emitter, 75 µm, tip: 8 ± 1 µm, New Objective; self-packed with Re- proSil-Pur 120 ODS-3, 3 µm, Dr. Maisch) using an aqueous-organic gradient (UltiMate 3000 HPLC coupled to a Velos Elite mass spectrometer (Thermo Scientific)). Full spectra (with precursor signals used for quantification) were acquired with a target value of 1,000,000 and a nominal resolution of 240,000 (scan range 370 to 1700 m/z). Up to ten data-dependent CID fragment spectra per scan cycle were acquired in the ion trap with a target value of 2000 and dynamic exclusion, preview mode for full precursor scans, charge state screening, monoisotopic precursor selection and rejection of charge state 1 enabled. The activation type was CID with the default settings. LC-MS/MS data were

extracted and searched for in the UniProt Knowledgebase (mouse, rat, human) using the Mascot search engine (Matrix Science). For preliminary searches, peptide mass tolerance was set to 15 ppm. After linear shift mass (omine) recalibration, the window was narrowed to  $\pm 5$  ppm for the final database searches. Fragment mass tolerance was set to 0.8 Da. One missed trypsin cleavage and common variable modifications were accepted for peptide identification (acetyl (protein N-term), carbamidomethyl (C) Gln $\rightarrow$ pyro-Glu (N-term Q), Glu $\rightarrow$ pyro- Glu (N-term E), oxidation (M), propionamide (C)). The expected ion score cut-off was 0.5, resulting in a target decoy-based peptide FDR below 10%. Proteins identified by only one specific MS/MS spectrum or representing exogenous contamination, such as keratins or immunoglobulins, were eliminated. The MS data were quantitatively evaluated using the label-free evaluation pipeline already described (Schwenk et al., 2014). Briefly, m/z features in the LC-MS scans were detected and their intensities integrated (as intensity  $\times$  retention time  $\times$  m/z width = peak volume; PV) using MaxQuant (Cox and Mann, 2008), version 1.4. The m/z-corrected features were then aligned between the LC-MS/MS runs and assigned to the peptides identified by Mascot using a home-written software tool with mass tolerance set to 1.5 ppm for MS/MS-identified peptides and a time shift window of 1 min. Based on these accurately assigned PVs, protein abundance ratios (rPVs) between samples/controls were determined using the TopCorr method (Bildl et al., 2012): protein-specific peptide PVs were ranked across the datasets evaluated by their consistency using pairwise linear correlation analysis (Pearson correlation). A maximum of six to a minimum of two peptide PVs were then selected from the best correlated PVs to calculate the protein abundance ratio as the median of the respective peptide PV ratios. To ensure validity, sequenced peptides lacking a PV assignment were omitted and a minimum of two peptide ratios with total assigned PVs of 80,000 intensity units were required; if no PV could be assigned to a peptide in the AP controls, the detection limit of the spectrometer (3000 PV units with the settings used here) was inserted as a minimum estimate. For each protein, the consistency of enrichment with the antibodies used and across datasets was evaluated as well as its abundance and quantitative correlation with the purified target.

#### *Patch clamp experiments on astrocytes*

Three days before the experiment, dB-cAMP-differentiated astrocytes were trypsinized and seeded at a density of  $1\text{--}3 \times 10^4$  cells onto 24-well plates containing a glass coverslip with supplemented DMEM and 250  $\mu\text{M}$  dBcAMP. For electrophysiological recordings, the glass coverslip was mounted on the stage of inverted microscopy equipped with phase-contrast optics and fluorescence illumination. Patch pipettes were pulled from borosilicate glass capillaries (Clark Electromedical, England) and used after fire polishing (Narishige, Japan). The electro-physiological recordings were performed with a patch clamp amplifier (Axopatch 200B, Molecular Devices, Union City, CA). The patch electrodes were fabricated in a Flaming/Brown micropipette puller P-97 (Sutter instruments). The electrodes had a resistance of 4–5 M $\Omega$  when filled with intracellular solution (in mM): 144 NMDG-Cl, 2 MgCl<sub>2</sub>, 5 EGTA, 5 HEPES, with pH 7.3 and  $308 \pm 2$  mOsm/kg. Hypotonic extracellular solution ( $\sim 25\%$ ) was obtained by decreasing the NMDG- Cl concentration to 105 mM ( $229 \pm 2$  mOsm/kg). The extracellular solution contained (in mM): 144 NMDG-Cl, 2 CaCl<sub>2</sub>, 2 MgCl<sub>2</sub>, 5 HEPES, 5 glucose, with pH 7.4 and  $310 \pm 3$  mOsm/kg. All the solution osmolarities were adjusted with sorbitol. An Ag/AgCl ground electrode mounted in a 3 M KCl agar bridge was used. Membrane currents were recorded in the whole-cell patch clamp configuration, filtered at 2 kHz, digitized at 10 kHz and acquired with pClamp 10 software (Molecular Devices). Data

were analysed with Clampfit 10 (Molecular Devices) and Prism 4 (GraphPad Software, Inc., La Jolla, CA). Whole-cell capacitance and series resistance were compensated with the amplifier circuitry.

Series resistance was always kept below 10 M $\Omega$  and compensated at 70%–80%. All recordings were performed at room temperature (22–23 °C). Currents were evoked in 4 s pulses from +80 or +50 mV to –120 mV from a holding potential of 0 mV, as indicated in each figure.

#### *Two-electrode voltage clamp in Xenopus oocytes*

For expression in *Xenopus* oocytes, after linearization by NotI, cRNA of human LRRC8 proteins was transcribed using the mMessage mMachine SP6 kit (Ambion). We produced cRNA of hLRRC8A/E-VFP and hLRRC8A/C/E-mCherry fluorescent constructs. They were co-ex- pressed or not with MLC1. After cRNA injection, the oocytes were kept at 18 °C in modified Barth's solution (in mM): 88 NaCl, 1 KCl, 0.41 CaCl<sub>2</sub>, 0.82 MgSO<sub>4</sub>, 0.33 Ca(NO<sub>3</sub>)<sub>2</sub>, 2.4 NaHCO<sub>3</sub>, 10 Hepes, with pH 7.4, containing 10 mg/ml of Gentamicin. One to three days after injection, voltage clamp measurements were taken using the CellWorks (npi) program and a Tec-05 $\times$  amplifier (npi electronics, Tamm, Germany).

#### *Cell culture, transfection and the split-TEV method*

HeLa cells were grown at 37 °C in an atmosphere of 5% CO<sub>2</sub> in DMEM (Sigma-Aldrich, St Louis, USA) supplemented with 1 mM sodium pyruvate, 2 mM L-glutamine, 100 U/ml streptomycin, 100 mg/ml penicillin and 5% (v/v) foetal bovine serum. The cells were seeded into plates containing or not poly-D-lysine-coated cover slips. The cells were transiently transfected with the corresponding cDNA constructs using Transfectin (Bio-Rad, Hercules, USA). The split-TEV assay was performed as previously described (Lopez-Hernandez et al., 2011b).

#### *Statistical analyses*

For each value calculated from the different experiments, the data indicated are the mean  $\pm$  SEM. Statistical analysis was performed using GraphPad prism software. To estimate statistical significance, for experiments comparing two populations, we used a two-tailed unpaired Student t-test. For experiments comparing three or more populations, we used one-way ANOVA with Bonferroni multiple-comparison tests. The test used is indicated in the legend of each of the figures.

## **Results**

### *VRAC currents depend on LRRC8A expression in astrocytes*

We first aimed to demonstrate unambiguously that VRAC currents in astrocytes depend on the expression of LRRC8 proteins as recently indicated (Formaggio et al., 2018). For this reason, we focused on LRRC8A: the main subunit of VRAC (Stauber, 2015). Thus, we developed adenoviral vectors expressing an shRNA against rat LRRC8A or a scrambled shRNA (SCR) expressing also the fluorescent protein EmGFP, as a control. In order to test the efficacy of the shRNA, we tested commercially available antibodies and also developed new ones against LRRC8A (see

Methods). To control the specificity of the antibodies, HAP1 LRRC8A<sup>-/-</sup> cells were used. Western blot analysis indicated that a commercially available antibody was suitable for detecting LRRC8A by this method in HAP1 cells and rat and mouse primary astrocytes (Fig. 1A), but not by immunofluorescence experiments. In contrast, our newly developed antibody could be used for immunofluorescence stainings, although it also labelled the nuclei non-specifically in both HAP1 wild-type (WT) and HAP1 LRRC8A<sup>-/-</sup> cells (Fig. 1B).

Western blot analysis performed 7 days after LRRC8A shRNA infection of astrocytes indicated that the LRRC8A protein level was reduced by 80% compared with control astrocytes or astrocytes transduced with an adenovirus expressing SCR shRNA (Fig. 2A). Immunofluorescence experiments confirmed that no detectable LRRC8A protein was present in the astrocytes transduced with an adenovirus expressing the LRRC8A shRNA (Fig. 2B), whereas LRRC8A was localized at the edges of the astrocyte membrane in cells transduced with SCR shRNA (Fig. 2B).

Previous studies have used dibutyryl-cAMP-differentiated astrocytes to investigate the role of GlialCAM and MLC1 in modulating VRAC currents (Capdevila-Nortes et al., 2013). VRAC currents have been measured previously in these differentiated astrocytes (Benfenati et al., 2007). To have only chloride currents in hypotonic conditions due to VRAC channels and not due to the ClC-2 channel, as previously performed (Capdevila-Nortes et al., 2013), we measured only chloride currents in hypotonic conditions in astrocytes that did not show ClC-2 currents in isotonic conditions (Fig. S1). Thus, dibutyryl-cAMP-differentiated astrocytes transduced with adenoviruses expressing LRRC8A shRNA were used for electrophysiological analyses to analyse the contribution of LRRC8A protein to VRAC currents. These experiments showed that LRRC8A silencing nearly abolished VRAC currents in hypotonic conditions (Scramble at +50 mV:  $17.6 \pm 5.3$  pA/pF, n = 5; LRRC8A shRNA:  $5.4 \pm 2.9$  pA/pF, n = 6; P < 0.05; Fig. 2C). This indicates that also in astrocytes, VRAC currents also depend on LRRC8 proteins, as already demonstrated in other cells (Wang et al., 2017) and recently also indicated in astrocytes (Formaggio et al., 2018). In agreement with this finding, astrocytes with reduced expression of LRRC8A displayed vacuolation (Fig. 1D), a phenotype that was previously observed in astrocytes inhibited with DCPIB (Capdevila-Nortes et al., 2013), a VRAC inhibitor (Decher et al., 2001), and also in kidney and other organs from *Lrrc8a*<sup>-/-</sup> mice (Kumar et al., 2014).

#### *Functional relationship between MLC1 and LRRC8A*

Previous works demonstrated reduced VRAC activity in rat astrocytes where MLC1 or GlialCAM expression was reduced by RNA interference (Capdevila-Nortes et al., 2013; Ridder et al., 2011). Similarly, primary astrocytes derived from two differently generated *Mlc1*<sup>-/-</sup> mouse lines showed reduced VRAC activity in one model (Dubey et al., 2015) and a slight, although not statistically significant decrease in the other (Sirisi et al., 2014). As experiments performed on one *Mlc1*<sup>-/-</sup> mice model used older primary astrocytes than those used in our model (Sirisi et al., 2014), we repeated these experiments on primary cultures of astrocytes with longer culture time. Thus, astrocytes remained in differentiation media for three weeks. In these experiments, we observed a statistically significant decrease of VRAC activity in *Mlc1*<sup>-/-</sup> astrocytes (Fig. 3A), thus further confirming that VRAC currents are reduced when MLC1 is absent.

It has been shown that in astrocytes overexpression of MLC1, but not of GlialCAM,

potentiates VRAC activity (Capdevila-Nortes et al., 2013). To confirm that MLC1 modulates LRRC8-mediated VRAC currents, we overexpressed MLC1 in astrocytes with a reduced expression of LRRC8A by RNA interference. In these cells, overexpression of MLC1 did not potentiate VRAC currents (Fig. 3B, C). Taken together, all these results suggest that MLC1 might regulate VRAC activity by acting on LRRC8 proteins in an undetermined way.

#### *In vitro studies analysing the biochemical and functional interaction between GlialCAM/MLC1 and LRRC8A*

As it has been shown that in astrocytes, GlialCAM/MLC1 directly modulates the activity of a chloride channel (ClC-2) (Sirisi et al., 2017), we reasoned that the same could occur with LRRC8 proteins. Therefore, we first established *in vitro* assays to study the possible interaction between LRRC8A, the main subunit of VRAC, and the GlialCAM/MLC1 complex. As a first approach, we measured the interaction between these proteins in transiently-transfected HeLa cells using the split-TEV assay (Capdevila-Nortes et al., 2012). In agreement with previous results indicating that MLC1, GlialCAM and LRRC8A homo-oligomerize (Estévez et al., 2018; Gaitán-Peñas et al., 2016), we confirmed MLC1, GlialCAM and LRRC8A homo-oligomerization by split-TEV (Fig. 4A). In contrast, the MLC1- or GlialCAM-LRRC8A hetero-oligomerization split-TEV signal was comparable to that of the negative controls (Fig. 4A), suggesting that these proteins do not interact directly.

We next explored whether GlialCAM/MLC1 could concentrate LRRC8A at cell-cell junctions, as demonstrated for ClC-2 (Gaitán-Peñas et al., 2017). For this purpose, we transiently expressed the three proteins in HeLa cells using the plasmids pCDNA3-LRRC8A-flag and pCDNA3-GlialCAM-E2A-MLC1, which allow the stoichiometric expression of both GlialCAM and MLC1. The flag tag does not interfere with LRRC8 function, as has been shown previously (Qiu et al., 2014). By performing cell immunostaining, we observed that both GlialCAM and MLC1 were present at cell-cell junctions (Fig. 4B). In contrast, immunostaining of LRRC8A showed an intracellular and a prominent membrane distribution, without co-localization with MLC1 or GlialCAM (Pearson correlation coefficients: GlialCAM/MLC1 = 0.89; MLC1/LRRC8A = 0.33) at cell-cell junctions (Fig. 4B).

Next, we considered whether the functional modulation of VRAC currents by GlialCAM/MLC1 observed in astrocytes may also occur in an *in vitro* system. To this aim, we used collagenase-treated *Xenopus* oocytes that have proved to be a valid expression system to study LRRC8 protein function (Gaitán-Peñas et al., 2018). Co-expression of MLC1, alone or together with GlialCAM, with fluorescently tagged LRRC8A and LRRC8C did not potentiate VRAC-mediated currents in *Xenopus* oocytes (Fig. 4C). Similar results were observed after co-expression of MLC1 with fluorescently tagged LRRC8A and LRRC8E (Fig. 4C).

#### *Biochemical studies of interactions between endogenous LRRC8A and GlialCAM/MLC1*

It is possible that the expression of these proteins in heterologous systems does not reflect the situation observed *in vivo*. So we analysed whether the LRRC8 and GlialCAM/MLC1 proteins could interact *in vivo*. We performed co-immunoprecipitation experiments of solubilized mouse brain extracts using a monoclonal antibody against

MLC1. Whereas the anti-MLC1 antibody was able to co-immunoprecipitate CIC-2 as previously shown (Sirisi et al., 2017), it failed to co-immunoprecipitate LRRC8A (Fig. 5A). Similarly, antibodies against GlialCAM failed to immunoprecipitate LRRC8A (not shown).

Then, we studied whether LRRC8A and MLC1 may co-localize in primary astrocytes, where functional modulation of VRAC by MLC1 has been observed. For this purpose, we simultaneously detected endogenous LRRC8A and MLC1 in mouse or rat primary astrocytes performing co-immunostaining using a monoclonal antibody against MLC1 and a polyclonal antibody against LRRC8A (Fig. 5B). As previously reported (Duarri et al., 2011), MLC1 was detected at rat astrocyte-astrocyte junctions, where it co-localizes with GlialCAM (Capdevila-Nortes et al., 2013). In contrast, we observed LRRC8A expression in the plasma membrane without showing any co-localization with MLC1 at cell-cell junctions (Pearson correlation coefficients: GlialCAM/MLC1 = 0.80; MLC1/LRRC8A = 0.01) (Fig. 5B).

Collectively, results obtained so far on endogenous and heterologously expressed proteins suggest that GlialCAM/MLC1 complex may modulate VRAC currents in astrocytes indirectly through unknown factors not present in *Xenopus* oocytes.

#### *Studying the mechanisms of GlialCAM/MLC1 modulation of VRAC*

In order to gain insight into how GlialCAM/MLC1 may modulate LRRC8A, we analysed LRRC8A expression in brain tissue and in cultured astrocytes derived from *Mlc1* KO animals (Hoegg-Beiler et al., 2014). First, we determined whether the lack of MLC1 affected LRRC8A mRNA levels using real-time PCR. No changes were observed when controls (WT) were compared with the *Mlc1* KO samples, either from total brain without cerebellum and from cerebellum, which is the region mainly affected by vacuolation in *Mlc1*<sup>-/-</sup> mice (Hoegg-Beiler et al., 2014) (Fig. 6A). Similarly, protein levels of LRRC8A did not change in the cerebellum of *Mlc1*<sup>-/-</sup> (Fig. 6B and Fig. S2), whereas in this region CIC-2 expression was previously found reduced (Hoegg-Beiler et al., 2014). In the same manner, comparison of LRRC8A protein levels between astrocytes obtained from WT and *Mlc1*<sup>-/-</sup> mice showed no differences (Fig. 6C and Fig. S2).

We also quantified the levels of LRRC8A in the plasma membrane in astrocytes isolated from WT and *Mlc1*<sup>-/-</sup> mice using surface biotinylation. Again, no differences in protein surface levels were detected between the two cell populations (Fig. 6D and Fig. S2). We also studied whether the lack of MLC1 influenced the localization of LRRC8A in primary astrocytes using immunofluorescence, but we did not observe any change, and LRRC8A was detected in the plasma membrane edges in both WT and *Mlc1* KO cells (Fig. 6E). No changes in total protein levels or subcellular localization of LRRC8A were observed in astrocytes isolated from *Glialcam* KO mice either (Figs. S2 and S3). In agreement with these results, no LRRC8A localization change was observed in vivo in the brain of *Glialcam* KO animals (Bugiani et al., 2017).

#### *Further evidence that MLC1 may modulate signal transduction cascades*

We then reasoned that the lack of MLC1 might affect VRAC by altering some signal transduction cascade important for its functional modulation. In fact, a recent report has shown that overexpression of MLC1 in a glial cell line reduces the activation of ERK by inhibiting their phosphorylation (Lanciotti et al., 2016). The same pathway has

previously been reported to modulate VRAC activity (Crepel et al., 1998; Pedersen et al., 2016). In the opposite way of MLC1 over-expression, here we observed an increase in ERK phosphorylation in primary astrocytes from *Mlc1*<sup>-/-</sup> mice when compared to WT cells, indicating that in these cells the activity of some signal transduction mediators vary as a function of MLC1 protein levels (Fig. 7A, B).

To establish whether VRAC has post-translational modifications that depend on MLC1, we immunoprecipitated LRRC8A from astrocytes overexpressing MLC1 (using adenoviruses expressing MLC1) and from astrocytes with a reduced expression of MLC1 (using adenoviruses expressing shRNA for MLC1). MS-analysed affinity-purified proteins detected all LRRC8 proteins, confirming the specificity of the immunoprecipitation. The proteomic analysis revealed the presence of phosphorylated peptides corresponding to the phosphorylation of two serines (serine 212 and 215) in the intracellular loop between the predicted second and third transmembrane domain (Abascal and Zardoya, 2012) of the LRRC8C accessory subunit (Fig. S4 and Fig. 7C). Using abundance-normalized values as an approximate measure of protein abundance, we could determine that the phosphorylation of these two serines was increased approximately tenfold in cells with a reduced expression of MLC1, compared with cells overexpressing MLC1 (Fig. 7D). These results suggest that MLC1 protein can favour VRAC functionality on signal transduction cascades modulating channel phosphorylation.

## Discussion

Previous results from our group and others have shown that lack of *Mlc1* or GlialCAM causes a reduction in the activity of two chloride channels (Bugiani et al., 2017; Dubey et al., 2015; Hoegg-Beiler et al., 2014; Ridder et al., 2011). On one hand, there is experimental evidence from animal models and cell cultures indicating that plasma membrane stability and localization and the activity of the ClC-2 chloride channel in glial cells can be modulated directly by GlialCAM and MLC1 (Gaitán-Peñas et al., 2017; Hoegg-Beiler et al., 2014; Jeworutzki et al., 2012). On the other hand, studies on cultured astrocytes have previously shown that the activity of VRAC is partially diminished when MLC1 expression is reduced (Capdevila-Nortes et al., 2013; Dubey et al., 2015; Ridder et al., 2011; Sirisi et al., 2014). Although it has been speculated that MLC1 might directly mediate VRAC currents (Ridder et al., 2011), the recent discovery that VRAC activity is mediated by LRRC8 proteins and the fact that VRAC currents are still present in astrocytes from *Mlc1*<sup>-/-</sup> mice, invalidated that hypothesis. Thus, the question is: How does GlialCAM/MLC1 modulate LRRC8-mediated VRAC currents?

The first finding of the present work is that, using novel tools and a multiplicity of experimental approaches, there is no physical interaction between LRRC8A, the main subunit of VRAC, and the GlialCAM/MLC1 complex. In fact, we have never, and neither has anyone else to the best of our knowledge, detected LRRC8 proteins among GlialCAM or MLC1 molecular interactors (Brignone et al., 2015; Lopez-Hernandez et al., 2011a; Sugio et al., 2017). Preliminary proteomic studies by our group using antibodies against LRRC8A have not detected GlialCAM or MLC1 as a LRRC8A interacting partner either. Furthermore, recent results using immunogold labeling have shown that LRRC8A is localized at the astrocytic endfeet membrane facing endothelial cells (Formaggio et al., 2018) and is not present at astrocyte-astrocyte junctions where MLC1 is localized, making a direct interaction nearly impossible. Thus, we believe that the modulation of VRAC by GlialCAM/MLC1 has to be completely different from what

observed for the CIC-2 chloride channel.

Thus, our studies have shown that there is no change in the levels of mRNA or the total and plasma membrane levels of LRRC8A protein when MLC1 expression is lost. In a recent study characterizing GlialCAM KO mice (Bugiani et al., 2017), it was shown that the sub-cellular localization of LRRC8A was not changed. However, we cannot conclude that LRRC8 proteins are not altered in MLC, since other LRRC8 parameters remain to be studied, as do those of the LRRC8 accessory subunits, such as the levels at the plasma membrane of the LRRC8 accessory subunits or even the degree of association of LRRC8A with the different LRRC8 accessory subunits.

Taking into account all these results, we conclude that the modulation of LRRC8 proteins by GlialCAM/MLC1 may be indirect. It has previously been shown that the VRAC activity could be regulated by multiple post-translational modifications such as phosphorylation or oxidation (Pedersen et al., 2015, 2016). In fact, ERK was involved in the activation of VRAC (Crepel et al., 1998; Pedersen et al., 2016) and recently it has been shown that overexpression of MLC1 affects signalling transduction pathways (Lanciotti et al., 2016). These results have been validated in this work, where we show changes in the opposite direction in ERK phosphorylation when MLC1 is absent. However, activation of ERK and tyrosine kinases have been previously related with the activation of VRAC during the administration of a hypotonic solution (Crepel et al., 1998) and here we find the opposite. Maybe, our results suggested that ERK can be involved also in the long term regulation of VRAC. In summary, we suggest that GlialCAM/MLC1 may regulate VRAC by affecting signal transduction mechanisms.

In agreement with this hypothesis, we found an increase in the phosphorylation of two serines in an intracellular loop of the VRAC accessory subunit LRRC8C when the expression of MLC1 is reduced. However, we cannot conclude that ERK phosphorylates directly LRRC8C, as it may be regulated by a different kinase/phosphatase. Studying how the modification of the phosphorylation of these two serines influences the activity of VRAC is not easy. Considering that the channel is formed by four accessory subunits with a non-fixed stoichiometry (Gaitán-Peñas et al., 2016), expressing a subunit may change the properties of the channel. In the recent structure of the homologous LRRC8A, these amino acids are not solved in the 3D structure (Deneka et al., 2018), but are probably far away from the pore. It could be speculated that this phosphorylation may influence the levels of LRRC8C at the plasma membrane or the association of LRRC8C with LRRC8A. As LRRC8C is a subunit that show a reduced inactivation (Stauber, 2015), influencing LRRC8C by phosphorylation may also influence inactivation. Further studies are needed to examine these hypothesis.

One important issue that remains to be clarified is the mechanism by which GlialCAM/MLC1 modulates signal transduction. Although the exact function of GlialCAM/MLC1 is still unknown, we have previously hypothesized (Estévez et al., 2018) that GlialCAM/MLC1 may work as a sensor of neuronal activity in glial cells (by detecting changes in voltage or potassium concentration) and thus coordinate a metabolic programme of different ion channels, transporters and other proteins by unknown mechanisms. The activity of these proteins may counteract the increases of extracellular potassium during high neuronal activity by increasing the uptake of potassium or by distributing potassium through the glial syncytium. Several proteins involved in potassium handling or volume regulation have been shown to be modulated

by GlialCAM/MLC1, such as CIC-2, VRAC, Na<sup>+</sup>/K<sup>+</sup>-ATPase, TRPV4 or connexin 43 (Estévez et al., 2018). In agreement with this hypothesis, a recent report has shown that there is disturbance of extracellular potassium upon neuronal activation in two MLC mice models (Dubey et al., 2018); this could explain the increase in seizures observed in MLC patients.

Among the proteins that are regulated by GlialCAM/MLC1, we have suggested (Hoegg-Beiler et al., 2014; Sirisi et al., 2017) that modulation of CIC-2 activity, which changes CIC-2 from an inwardly-rectifying to an ohmic channel, will allow chloride influx at depolarized potentials. This could contribute to enhanced potassium uptake by compensating potassium-dependent positive charges, as already previously suggested (Blanz et al., 2007). Meanwhile, all these ion fluxes lead to water flux causing astrocyte swelling and VRAC activation. The activation of VRAC by GlialCAM/MLC1 may be very important to prevent this swelling and release water. If VRAC is not working properly, water may remain in glial cells, which may encapsulate it into vacuoles. In fact, vacuoles have been observed in many cell types after *Lrrc8a* disruption (Kumar et al., 2014). A defect in VRAC activity may also contribute to a reduction in the capacity of astrocytes to uptake potassium.

In summary, the present work confirms previous suggestions that GlialCAM/MLC1 may modulate different proteins by changing signal transduction mechanisms in a direct or indirect manner, such as the LRRC8/VRAC studied here. Understanding how GlialCAM/MLC1 influences signal transduction processes is one of the keys to envisaging and developing therapeutic strategies for MLC patients.

#### **Conflict of interest statement**

The authors declare no competing financial interests.

#### **Acknowledgements**

This work was supported in part by: the European Leukodystrophies Association (ELA) Research Foundation (ELA2012-014C2B to RE and VN); the Spanish Ministerio de Ciencia e Innovación (MICINN) (SAF2015- 70377 to RE); the Generalitat de Catalunya (SGR2014-1178 to RE, 2017SGR737 to XG and SGR2014-541 to VN); the Instituto de Salud Carlos III (organism linked to MICINN and FEDER), (ERARE to RE, RETIC RD16/0008/0014 to XG, FISPI17/00296 to XG and FIS PI16/00267-R-FEDER to VN). RE is a recipient of an ICREA Academia prize. We thank Thomas J Jentsch for the gift of the *Glialcam*<sup>-/-</sup> colony, L. González for colony management and Esther Adanero for technical support. We also thank Uwe Schulte for critical reading of the manuscript.

#### **References**

Abascal, F., Zardoya, R., 2012. LRRC8 proteins share a common ancestor with pannexins, and may form hexameric channels involved in cell-cell communication. *BioEssays* 34, 551–560.

Barrallo-Gimeno, A., Gradogna, A., Zanardi, I., Pusch, M., Estévez, R., 2015. Regulatory-auxiliary subunits of CLC chloride channel-transport proteins. *J. Physiol.* 593, 4111–4127.

Benfenati, V., Nicchia, G.P., Svelto, M., Rapisarda, C., Frigeri, A., Ferroni, S., 2007.

Functional down-regulation of volume-regulated anion channels in AQP4 knockdown cultured rat cortical astrocytes. *J. Neurochem.* 100, 87–104.

Bildl, W., Haupt, A., Müller, C.S., Biniossek, M.L., Thumfart, J.O., Hüber, B., Fakler, B., Schulte, U., 2012. Extending the dynamic range of label-free mass spectrometric quantification of affinity purifications. *Mol. Cell. Proteomics* 11 (M1111.007955).

Blanz, J., Schweizer, M., Auberson, M., Maier, H., Muenscher, A., Hubner, C.A., Jentsch, T.J., 2007. Leukoencephalopathy upon disruption of the chloride channel CIC-2. *J. Neurosci.* 27, 6581–6589.

Brignone, M.S., Lanciotti, A., Macioce, P., Macchia, G., Gaetani, M., Aloisi, F., Petrucci, T.C., Ambrosini, E., 2011. The beta1 subunit of the Na,K-ATPase pump interacts with megalencephalic leukoencephalopathy with subcortical cysts protein 1 (MLC1) in brain astrocytes: new insights into MLC pathogenesis. *Hum. Mol. Genet.* 20, 90–103.

Brignone, M.S., Lanciotti, A., Visentin, S., De Noció, C., Molinari, P., Camerini, S., Diociaiuti, M., Petrini, S., Minnone, G., Crescenzi, M., Laudiero, L.B., Bertini, E., Petrucci, T.C., Ambrosini, E., 2014. Megalencephalic leukoencephalopathy with subcortical cysts protein-1 modulates endosomal pH and protein trafficking in astrocytes: relevance to MLC disease pathogenesis. *Neurobiol. Dis.* 66, 1–18.

Brignone, M.S., Lanciotti, A., Camerini, S., De Nuccio, C., Petrucci, T.C., Visentin, S., Ambrosini, E., 2015. MLC1 protein: a likely link between leukodystrophies and brain channelopathies. *Front. Cell. Neurosci.* 09, 66.

Bugiani, M., Dubey, M., Breur, M., Postma, N.L., Dekker, M.P., ter Braak, T., Boschert, U., Abbink, T.E.M., Mansvelter, H.D., Min, R., van Weering, J.R.T., van der Knaap, M.S., 2017. Megalencephalic leukoencephalopathy with cysts: the Glialcam-null mouse model. *Ann. Clin. Transl. Neurol.* 4, 450–465.

Capdevila-Nortes, X., Lopez-Hernandez, T., Ciruela, F., Estevez, R., 2012. A modification of the split-tobacco etch virus method for monitoring interactions between membrane proteins in mammalian cells. *Anal. Biochem.* 423, 109–118.

Capdevila-Nortes, X., López-Hernández, T., Apaja, P.M., López de Heredia, M., Sirisi, S., Callejo, G., Arnedo, T., Nunes, V., Lukacs, G.L., Gasull, X., Estévez, R., 2013. Insights into MLC pathogenesis: GlialCAM is an MLC1 chaperone required for proper activation of volume-regulated anion currents. *Hum. Mol. Genet.* 22, 4405–4416.

Capdevila-Nortes, X., Jeworutzki, E., Elorza-Vidal, X., Barrallo-Gimeno, A., Pusch, M., Estévez, R., 2015. Structural determinants of interaction, trafficking and function in the CIC-2/MLC1 subunit GlialCAM involved in leukodystrophy. *J. Physiol.* 593, 4165–4180.

Cox, J., Mann, M., 2008. MaxQuant enables high peptide identification rates, individualized p.p.b.-range mass accuracies and proteome-wide protein quantification. *Nat. Biotechnol.* 26, 1367–1372.

Crepel, V., Panenka, W., Kelly, M.E., MacVicar, B.A., 1998. Mitogen-activated protein and tyrosine kinases in the activation of astrocyte volume-activated chloride current. *J. Neurosci.* 18, 1196–1206.

De Stefano, N., Balestri, P., Dotti, M.T., Grosso, S., Mortilla, M., Morgese, G., Federico,

A., 2001. Severe metabolic abnormalities in the white matter of patients with vacuolating megalencephalic leukoencephalopathy with subcortical cysts. A proton MR spectroscopic imaging study. *J. Neurol.* 248, 403–409.

Decher, N., Lang, H.J., Nilius, B., Brüggemann, A., Busch, A.E., Steinmeyer, K., Brüggemann, A., Busch, A.E., Steinmeyer, K., 2001. DCPIB is a novel selective blocker of I(Cl,swell) and prevents swelling-induced shortening of guinea-pig atrial action potential duration. *Br. J. Pharmacol.* 134, 1467–1479.

Deneka, D., Sawicka, M., Lam, A.K.M., Paulino, C., Dutzler, R., 2018. Structure of a volume-regulated anion channel of the LRRC8 family. *Nature*. <https://doi.org/10.1038/s41586-018-0134-y>. Depienne, C., Bugiani, M., Dupuits, C., Galanaud, D., Touitou, V., Postma, N., van Berkel, C., Polder, E., Tollard, E., Darios, F., Brice, A., de Die-Smulders, C.E., Vles, J.S., Vanderver, A., Uziel, G., Yalcinkaya, C., Frints, S.G., Kalscheuer, V.M., Klooster, J., Kamermans, M., Abbink, T.E., Wolf, N.I., Sedel, F., van der Knaap, M.S., 2013. Brain white matter oedema due to CLC-2 chloride channel deficiency: an observational analytical study. *Lancet Neurol.* 12, 659–668.

van der Knaap, M.S., Depienne, C., Sedel, F., Abbink, T.E.M., 1993. CLCN2-Related leukoencephalopathy. In: *GeneReviews(R)*. University of Washington, Seattle.

van der Knaap, M.S., Barth, P.G., Vrensen, G.F., Valk, J., 1996. Histopathology of an infantile-onset spongiform leukoencephalopathy with a discrepantly mild clinical course. *Acta Neuropathol.* 92, 206–212.

van der Knaap, M.S., Boor, I., Estevez, R., 2012. Megalencephalic leukoencephalopathy with subcortical cysts: chronic white matter oedema due to a defect in brain ion and water homeostasis. *Lancet Neurol.* 11, 973–985. [https://doi.org/10.1016/S1474-4422\(12\)70192-8](https://doi.org/10.1016/S1474-4422(12)70192-8).

Duarri, A., Lopez de Heredia, M., Capdevila-Nortes, X., Ridder, M.C., Montolio, M., Lopez-Hernandez, T., Boor, I., Lien, C.F., Hagemann, T., Messing, A., Gorecki, D.C., Scheper, G.C., Martinez, A., Nunes, V., van der Knaap, M.S., Estevez, R., 2011. Knockdown of MLC1 in primary astrocytes causes cell vacuolation: a MLC disease cell model. *Neurobiol. Dis.* 43, 228–238.

Dubey, M., Bugiani, M., Ridder, M.C., Postma, N.L., Brouwers, E., Polder, E., Jacobs, J.G., Baayen, J.C., Klooster, J., Kamermans, M., Aardse, R., de Kock, C.P.J., Dekker, M.P., van Weering, J.R.T., Heine, V.M., Abbink, T.E.M., Scheper, G.C., Boor, I., Lodder, J.C., Mansvelder, H.D., van der Knaap, M.S., 2015. Mice with megalencephalic leukoencephalopathy with cysts: a developmental angle. *Ann. Neurol.* 77, 114–131.

Dubey, M., Brouwers, E., Hamilton, E.M.C., Stiedl, O., Bugiani, M., Koch, H., Kole, M.H.P., Boschert, U., Wykes, R.C., Mansvelder, H.D., van der Knaap, M.S., Min, R., 2018. Seizures and disturbed brain potassium dynamics in the leukodystrophy megalencephalic leukoencephalopathy with subcortical cysts. *Ann. Neurol.* 83, 636–649.

Estévez, R., Elorza-Vidal, X., Gaitán-Peñas, H., Pérez-Rius, C., Armand-Ugón, M., Alonso-Gardón, M., Xicoy-Espauella, E., Sirisi, S., Arnedo, T., Capdevila-Nortes, X., López-Hernández, T., Montolio, M., Duarri, A., Tejjido, O., Barrallo-Gimeno, A., Palacín, M., Nunes, V., 2018. Megalencephalic leukoencephalopathy with subcortical

cysts: a personal biochemical retrospective. *Eur. J. Med. Genet.* 61, 50–60.

Ferroni, S., Marchini, C., Nobile, M., Rapisarda, C., 1997. Characterization of an inwardly rectifying chloride conductance expressed by cultured rat cortical astrocytes. *Glia* 21, 217–227.

Formaggio, F., Saracino, E., Mola, M.G., Rao, S.B., Amiry-Moghaddam, M., Muccini, M., Zamboni, R., Nicchia, G.P., Caprini, M., Benfenati, V., 2018. LRRC8A is essential for swelling-activated chloride current and for regulatory volume decrease in astrocytes. *FASEB J.* <https://doi.org/10.1096/fj.201701397RR>.

Gaitán-Peñas, H., Gradogna, A., Laparra-Cuervo, L., Solsona, C., Fernández-Dueñas, V., Barrallo-Gimeno, A., Ciruela, F., Lakadamyali, M., Pusch, M., Estévez, R., 2016. Investigation of LRRC8-Mediated Volume-Regulated Anion Currents in *Xenopus* Oocytes. *Biophys. J.* 111, 1429–1443.

Gaitán-Peñas, H., Apaja, P.M., Arnedo, T., Castellanos, A., Elorza-Vidal, X., Soto, D., Gasull, X., Lukacs, G.L., Estévez, R., 2017. Leukoencephalopathy-causing CLCN2 mutations are associated with impaired Cl<sup>-</sup> channel function and trafficking. *J. Physiol.* 595, 6993–7008.

Gaitán-Peñas, H., Pusch, M., Estévez, R., 2018. Expression of LRRC8/VRAC currents in *Xenopus* oocytes: advantages and caveats. *Int. J. Mol. Sci.* <https://doi.org/10.3390/ijms19030719>.

Hoegg-Beiler, M.B., Sirisi, S., Orozco, I.J., Ferrer, I., Hohensee, S., Auberson, M., Gödde, K., Vilches, C., de Heredia, M.L., Nunes, V., Estévez, R., Jentsch, T.J., 2014. Disrupting MLC1 and GlialCAM and CIC-2 interactions in leukodystrophy entails glial chloride channel dysfunction. *Nat. Commun.* 5, 3475.

Hyzinski-García, M.C., Rudkouskaya, A., Mongin, A.A., 2014. LRRC8A protein is indispensable for swelling-activated and ATP-induced release of excitatory amino acids in rat astrocytes. *J. Physiol.* 592, 4855–4862.

Jentsch, T.J., 2016. VRACs and other ion channels and transporters in the regulation of cell volume and beyond. *Nat. Rev. Mol. Cell Biol.* 17, 293–307.

Jeworutzki, E., Lopez-Hernandez, T., Capdevila-Nortes, X., Sirisi, S., Bengtsson, L., Montolio, M., Zifarelli, G., Arnedo, T., Muller, C.S., Schulte, U., Nunes, V., Martinez, A., Jentsch, T.J., Gasull, X., Pusch, M., Estevez, R., 2012. GlialCAM, a protein defective in a leukodystrophy, serves as a CIC-2 Cl<sup>-</sup> channel auxiliary subunit. *Neuron* 73, 951–961.

Jeworutzki, E., Lagostena, L., Elorza-Vidal, X., López-Hernández, T., Estévez, R., Pusch, M., 2014. GlialCAM, a CLC-2 Cl<sup>-</sup> channel subunit, activates the slow gate of CLC chloride channels. *Biophys. J.* 107, 1105–1116.

Kofuji, P., Newman, E.A., 2004. Potassium buffering in the central nervous system. *Neuroscience* 129, 1045–1056.

Kumar, L., Chou, J., Yee, C.S.K., Borzutzky, A., Vollmann, E.H., von Andrian, U.H.,

Park, S.-Y., Hollander, G., Manis, J.P., Poliani, P.L., Geha, R.S., 2014. Leucine-rich repeat containing 8A (LRRC8A) is essential for T lymphocyte development and function. *J. Exp. Med.* 211, 929–942.

Kunzelmann, K., 2015. TMEM16, LRRC8A, bestrophin: chloride channels controlled by Ca(2+) and cell volume. *Trends Biochem. Sci.* 40, 535–543.

Lanciotti, A., Brignone, M.S., Molinari, P., Visentin, S., De Nuccio, C., Macchia, G., Aiello, C., Bertini, E., Aloisi, F., Petrucci, T.C., Ambrosini, E., 2012. Megalencephalic leu-koencephalopathy with subcortical cysts protein 1 functionally cooperates with the TRPV4 cation channel to activate the response of astrocytes to osmotic stress: dysregulation by pathological mutations. *Hum. Mol. Genet.* 21, 2166–2180.

Lanciotti, A., Brignone, M.S., Visentin, S., De Nuccio, C., Catacuzzeno, L., Mallozzi, C., Petrini, S., Caramia, M., Veroni, C., Minnone, G., Bernardo, A., Franciolini, F., Pessia, M., Bertini, E., Petrucci, T.C., Ambrosini, E., 2016. Megalencephalic leukoencephalopathy with subcortical cysts protein-1 regulates epidermal growth factor receptor signaling in astrocytes. *Hum. Mol. Genet.* 25, 1543–1558.

Leegwater, P.A., Yuan, B.Q., van der Steen, J., Mulders, J., Konst, A.A., Boor, P.K., Mejaski-Bosnjak, V., van der Maarel, S.M., Frants, R.R., Oudejans, C.B., Schutgens, R.B., Pronk, J.C., van der Knaap, M.S., 2001. Mutations of MLC1 (KIAA0027), encoding a putative membrane protein, cause megalencephalic leukoencephalopathy with subcortical cysts. *Am. J. Hum. Genet.* 68, 831–838.

Lopez-Hernandez, T., Ridder, M.C., Montolio, M., Capdevila-Nortes, X., Polder, E., Sirisi, S., Duarri, A., Schulte, U., Fakler, B., Nunes, V., Scheper, G.C., Martinez, A., Estevez, R., van der Knaap, M.S., 2011a. Mutant GlialCAM causes megalencephalic leu-koencephalopathy with subcortical cysts, benign familial macrocephaly, and macrocephaly with retardation and autism. *Am. J. Hum. Genet.* 88, 422–432.

Lopez-Hernandez, T., Sirisi, S., Capdevila-Nortes, X., Montolio, M., Fernandez-Duenas, V., Scheper, G.C., van der Knaap, M.S., Casquero, P., Ciruela, F., Ferrer, I., Nunes, V., Estevez, R., 2011b. Molecular mechanisms of MLC1 and GLIALCAM mutations in megalencephalic leukoencephalopathy with subcortical cysts. *Hum. Mol. Genet.* 20, 3266–3277.

Pandey, A., Andersen, J.S., Mann, M., 2000. Use of mass spectrometry to study signaling pathways. *Sci. STKE* 2000 (37) (20 Jun, pp. p11).

Pasantes-Morales, H., Lezama, R.A., Ramos-Mandujano, G., Tuz, K.L., 2006. Mechanisms of cell volume regulation in hypo-osmolality. *Am. J. Med.* 119, S4–11.

Pedersen, S.F., Klausen, T.K., Nilius, B., 2015. The identification of a volume-regulated anion channel: an amazing Odyssey. *Acta Physiol (Oxford)* 213, 868–881.

Pedersen, S.F., Okada, Y., Nilius, B., 2016. Biophysics and physiology of the Volume-Regulated Anion Channel (VRAC)/Volume-Sensitive Outwardly Rectifying Anion Channel (VSOR). *Pflugers Arch.* 468, 371–383.

Qiu, Z., Dubin, A.E., Mathur, J., Tu, B., Reddy, K., Miraglia, L.J., Reinhardt, J., Orth,

A.P., Patapoutian, A., 2014. SWELL1, a plasma membrane protein, is an essential component of volume-regulated anion channel. *Cell* 157, 447–458.

Ridder, M.C., Boor, I., Lodder, J.C., Postma, N.L., Capdevila-Nortes, X., Duarri, A., Brussaard, A.B., Estevez, R., Scheper, G.C., Mansvelder, H.D., van der Knaap, M.S., 2011. Megalencephalic leukoencephalopathy with cysts: defect in chloride currents and cell volume regulation. *Brain* 134, 3342–3354.

Schober, A.L., Wilson, C.S., Mongin, A.A., 2017. Molecular composition and heterogeneity of the LRRC8-containing swelling-activated osmolyte channels in primary rat astrocytes. *J. Physiol.* 595, 6939–6951.

Schwenk, J., Baehrens, D., Haupt, A., Bildl, W., Boudkkazi, S., Roeper, J., Fakler, B., Schulte, U., 2014. Regional diversity and developmental dynamics of the AMPA-receptor proteome in the mammalian brain. *Neuron* 84, 41–54.

Sirisi, S., Folgueira, M., López-Hernández, T., Minieri, L., Pérez-Rius, C., Gaitán-Peñas, H., Zang, J., Martínez, A., Capdevila-Nortes, X., De La Villa, P., Roy, U., Alia, A., Neuhaus, S., Ferroni, S., Nunes, V., Estévez, R., Barrallo-Gimeno, A., 2014. Megalencephalic leukoencephalopathy with subcortical cysts protein 1 regulates glial surface localization of GLIALCAM from fish to humans. *Hum. Mol. Genet.* 23, 5069–5086.

Sirisi, S., Elorza-Vidal, X., Arnedo, T., Armand-Ugón, M., Callejo, G., Capdevila-Nortes, X., López-Hernández, T., Schulte, U., Barrallo-Gimeno, A., Nunes, V., Gasull, X., Estévez, R., 2017. Depolarization causes the formation of a ternary complex between GlialCAM, MLC1 and CIC-2 in astrocytes: implications in megalencephalic leukoencephalopathy. *Hum. Mol. Genet.* 26, 2436–2450.

Stauber, T., 2015. The volume-regulated anion channel is formed by LRRC8 heteromers –molecular identification and roles in membrane transport and physiology. *Biol. Chem.* 396, 975–990.

Sugio, S., Tohyama, K., Oku, S., Fujiyoshi, K., Yoshimura, T., Hikishima, K., Yano, R., Fukuda, T., Nakamura, M., Okano, H., Watanabe, M., Fukata, M., Ikenaka, K., Tanaka, K.F., 2017. Astrocyte-mediated infantile-onset leukoencephalopathy mouse model. *Glia* 65, 150–168.

Syeda, R., Qiu, Z., Dubin, A.E., Murthy, S.E., Florendo, M.N., Mason, D.E., Mathur, J., Cahalan, S.M., Peters, E.C., Montal, M., Patapoutian, A., 2016. LRRC8 Proteins Form Volume-Regulated Anion Channels that Sense Ionic Strength. *Cell* 164, 499–511.

Tejjido, O., Martinez, A., Pusch, M., Zorzano, A., Soriano, E., Del Rio, J.A., Palacin, M., Estevez, R., 2004. Localization and functional analyses of the MLC1 protein involved in megalencephalic leukoencephalopathy with subcortical cysts. *Hum. Mol. Genet.* 13, 2581–2594.

Voss, F.K., Ullrich, F., Münch, J., Lazarow, K., Lutter, D., Mah, N., Andrade-Navarro, M.A., von Kries, J.P., Stauber, T., Jentsch, T.J., 2014. Identification of LRRC8 heteromers as an essential component of the volume-regulated anion channel VRAC. *Science* 344, 634–638.

Wang, R., Lu, Y., Gunasekar, S., Zhang, Y., Benson, C.J., Chapleau, M.W., Sah, R., Abboud, F.M., 2017. The volume-regulated anion channel (LRRC8) in nodose neurons is sensitive to acidic pH. *JCI Insight* 2, e90632.

Wu, M., Moh, M.C., Schwarz, H., 2016. HepaCAM associates with connexin 43 and enhances its localization in cellular junctions. *Sci. Rep.* 6, 36218.

## Figure legends

### *Fig. 1. Validation of anti-LRRC8A antibodies used.*

A. Western blot of a commercially available (left) anti-LRRC8A antibody (Bethyl Laboratories, Montgomery, USA) and a newly developed antibody (right), using actin as a loading control. Protein extracts were obtained from WT HAP1 or LRRC8A<sup>-/-</sup> HAP1 cells (Invitrogen), rat and mouse primary astrocytes. In astrocytes, the lane indicates 95 kDa. Better LRRC8A detection was obtained with the commercially available antibody. B. Immunofluorescence detection of LRRC8A using two different anti-LRRC8A antibodies (green). Nuclei were stained with DAPI (blue). No specific signal was observed for the commercially available antibody. In contrast, the newly developed anti-LRRC8A antibody detected membrane edges (arrows) in WT but not in LRRC8A<sup>-/-</sup> HAP1 cells. The antibody also detected the cell nuclei non-specifically. These are typical results from two independent experiments. Scale bar: 20  $\mu$ m.

### *Fig. 2. LRRC8A is crucial for VRAC activity in primary rat astrocytes.*

A. (Left) Western blot of LRRC8A protein in astrocyte control (Ctrl), astrocytes transduced with adenovirus expressing and SCR shRNA (SCR) or expressing an shRNA against LRRC8A (LRRC8A shRNA). Actin was used as a loading control. (Right) Densitometric analysis detected that the mean percentage of LRRC8A protein levels was  $17.8\% \pm 6.2\%$  of SCR astrocytes ( $n = 3$ ). B. Immunofluorescence assay of LRRC8A detection in SCR- (left) or LRRC8A shRNA- (right) transduced rat astrocytes. These are typical images from four independent experiments. Arrows point to the LRRC8A antibody signal detected in membrane edges. Scale bar: 20  $\mu$ m. C. Representative traces of whole-cell chloride currents in dbcAMP-treated primary mouse astrocytes transduced with adenoviruses expressing scrambled shRNA (Scr), or shRNA for LRRC8A. We selected astrocytes that did not show CIC-2 currents in isotonic conditions (approximately 55%). In about 85% of these cells do not having CIC-2 currents in isotonic conditions, application of a hypotonic solution activated VRAC current. Data were recorded in isotonic conditions (top row) and after 5 min in a hypotonic medium (bottom row). Hyperpolarizing or depolarizing pulses from  $-120$  to  $+50$  mV were applied from a holding voltage of 0 mV. D. Astrocytes were stained with calcein to visualize vacuoles. Quantification of the percentage of cells displaying vacuolization showed increased number of cells with vacuoles in LRRC8A-depleted astrocytes ( $n = 4$ ;  $P \leq 0.01$  in two-tailed Student t-test). Cells showing vacuolization were defined as a cell having at least three vacuoles of a size bigger than 0.5  $\mu$ m.

### *Fig. 3. Modulation of LRRC8/VRAC-dependent currents by GlialCAM/MLC1 in mouse and primary astrocytes.*

A. Left: Representative traces of whole-cell VRAC currents in dbcAMP-treated primary astrocytes from WT or Mlc1 KO mice activated after 5 min in a hypotonic medium. Hyperpolarizing or depolarizing pulses from  $-120$  to  $+80$  mV were applied from a holding voltage of 0 mV, as shown. Right: Quantification of VRAC currents at  $-120$  mV

in isotonic and hypotonic conditions in WT (n = 11) and MLC1 KO (n = 11) primary astrocytes. \*P = 0.0204 vs. WT hypotonic. B. Average current–voltage relationship of VRAC currents activated by hypotonicity in transduced rat astrocytes with adenoviruses expressing scrambled shRNA (SCR; empty circles, n = 5), astrocytes transduced with adenoviruses expressing shRNA for LRRC8A (shLRRC8A; black circles; n = 7), astrocytes transduced with adenoviruses expressing MLC1 (MLC1; grey circles, n = 8) and astrocytes transduced with adenoviruses expressing shRNA for LRRC8A and adenoviruses expressing MLC1 (miLRCC8A + MLC1; light grey circles; n = 6). C. Quantification of the VRAC currents at -120 and + 50 mV in hypotonic conditions in the astrocytes shown in B. Significant statistical differences were found between scrambled astrocytes and miLRRC8A (\*P = 0.041) or MLC1 (\*P = 0.048). No significant statistical difference was found between scrambled astrocytes and miLRCC8A + MLC1 (P = 0.035).

*Fig. 4. In vitro studies of MLC1/GlialCAM-LRRC8 biochemical and functional interactions.*

A. Results of split-TEV interaction assays using LRRC8A (left) C-terminally tagged with the N terminal part of the TEV protease (TevSpA) or MLC1 and GlialCAM tagged in a similar manner. They were co-transfected with different constructs (LRRC8A, MLC1, and A2AR (adenosine receptor), as a negative control) C-terminally tagged with the C terminal part of the TEV protease. Interaction was measured as described in Material and methods. n = 4; \*\*\*P < 0.001, ns: not-significant comparing the interaction of each group to the interaction with the negative control in Bonferroni's multiple comparison test. B. Immunofluorescence detection of C-terminally flag-tagged LRRC8A (green) and MLC1 (red) in transiently transfected HeLa cells with pCDNA3 GlialCAM-E2A-MLC1 and pCDNA3 LRRC8A-flag. Nuclei were stained with DAPI (blue). Arrows point to cell-cell junctions. Scale bar: 20  $\mu$ m. C. In vitro current recordings in the *Xenopus* oocyte expression system. In vitro transcribed cRNAs from fluorescent-tagged LRRC8 family members (as indicated) were co-injected into the *Xenopus* oocyte with or without MLC1. Current intensities induced by co-expressing 8A-VFP plus 8C-mCherry, or 8E-mCherry plus or not MLC1, are compared as indicated (bottom panel). Current intensity values at +70 mV were normalized to the mean value of 8A-VFP plus 8C/8E-mCherry in the absence of MLC1. Data represent the mean  $\pm$  SEM from three-four independent experiments with 2 different cRNA preparations. ns: not-significant comparing with the group without MLC1.

*Fig. 5. Co-localization and interaction studies of endogenous LRRC8A with GlialCAM/MLC1.*

A. Immunoprecipitation of MLC1 from solubilized mouse brain extracts (Sol) using an anti-MLC1 monoclonal antibody coupled to Sepharose-A beads (IP MLC1). Uncoupled beads were used as a negative control (IP -). The SN of both purifications is included. The proteins detected by Western blot were MLC1 (to prove that MLC1 was purified), CIC-2 (as a protein that forms a ternary complex with MLC1) and LRRC8A. Another experiment gave similar results. B. Immunofluorescence co-labelling of LRRC8A (red) and MLC1 (green). Nuclei were stained with DAPI (blue). These are typical images from three independent experiments. MLC1 was present at rat astrocyte-astrocyte junctions (arrows), whereas LRRC8A was detected in membrane edges but not at the junctions. Scale bar: 20  $\mu$ m.

*Fig. 6. LRRC8A biochemical characterization in Mlc1 KO mice.*

A. Ratio of LRRC8A mRNA expression levels in the brain and cerebellum of WT versus

Mlc1<sup>-/-</sup> mice measured by qPCR revealed no significant differences between the two conditions.  $P = 0.315$  for ko brains vs WT ( $n = 3$  ko,  $n = 3$  wt) and  $P = 0.416$  for ko cerebellums vs WT ( $n = 3$  ko,  $n = 3$  wt). B. Western blot of LRRC8A protein levels in membrane extracts from WT and Mlc1<sup>-/-</sup> mice. MLC1 is tested to verify that it was not present in samples from Mlc1<sup>-/-</sup> mice and actin was used as a loading control. No differences in protein levels (after actin correction) were found ( $n = 6$ ;  $P = 0.15$  (cerebellum) in a two-tailed Student t-test of WT vs Mlc1<sup>-/-</sup>). C. Western blot of LRRC8A protein levels in cultured astrocytes. No differences in protein levels were found ( $n = 4$ ;  $P = 0.34$  in a two-tailed Student t-test of WT vs Mlc1<sup>-/-</sup>). D. Surface biotinylation of WT and Mlc1<sup>-/-</sup> astrocytes. Aliquots of solubilized extracts (Sol), SN of the purification and pellet of the purification (P) were analysed by Western blot using anti-LRRC8A or anti-MLC1 antibodies. Calnexin (a protein resident in the endoplasmic reticulum) was tested for to prove that intracellular membrane proteins were not present in the pellet fraction. E. Immunofluorescence of LRRC8A in WT (left) or Mlc1<sup>-/-</sup> (right) primary mouse quiescent astrocytes. These are typical images from four different experiments. LRRC8A was detected in cell membrane edges (arrowheads), and no apparent differences in localization were observed between the two groups.

*Fig. 7. Signal transduction changes observed in astrocytes dependent on MLC1 expression.*

A. Western blot analysis of protein extracts derived from Mlc1<sup>-/-</sup> and WT mice astrocytes indicated an increase in p-ERK protein in Mlc1<sup>-/-</sup> mice astrocytes. ERK was constant and was used as a loading control. Molecular weight markers (kDa) are indicated on the left side of the panels. B. Densitometric analysis of phosphorylated ERK/total ERK protein bands. Means  $\pm$  SEM of ten experiments are shown ( $*P < 0.05$ ). C. Mass spectrometric analysis of LRRC8A-associated VRAC complexes affinity-purified from solubilized rat astrocyte membranes which either overexpress MLC1 (MLC1<sup>++</sup>) or are endogenous MLC1 knocked down (MLC1<sup>kd</sup>) by shRNA. CID-MS/MS spectrum showing the fragmentation pattern of the bona fide double-phosphorylated peptide identified, SSQLKSIPEK, in two independent MS/MS spectra from anti-LRRC8A AP from MLC1<sup>kd</sup>. D. Mass traces and XICs (area-under-curve signal intensities) of that peptide in MLC1<sup>++</sup> (red, mass range 638.7782–638.7889 a.u.) and MLC1<sup>kd</sup> (blue, mass range 678.7782–678.7884 a.u.).